Electronic Supporting Information (ESI)

Surface functionalization of polyoxovanadium clusters: Generation of highly soluble charge carriers for nonaqueous energy storage

Lauren E. VanGelder[a], Harry D. Pratt III,[b] Travis M. Anderson, [b] and Ellen M. Matson *[a]

[a]Department of Chemistry, University of Rochester, Rochester, New York 14627

[b]Sandia National Laboratories, Albuquerque, NM 87185, USA.

Corresponding author email: matson@chem.rochester.edu

Table of Contents:

Experimental Methods.

General Considerations. Manipulations that required the absence of water and oxygen were conducted in a UniLab MBraun inert atmosphere glovebox under a dinitrogen atmosphere. Glassware was oven dried for a minimum of 4 hours and cooled in an evacuated antechamber prior to use in the drybox. Anhydrous methanol, ethanol, propanol, butanol, pentanol, hexanol, 2-methoxy ethanol, and 2-ethoxy ethanol were purchased from Sigma-Aldrich and stored over activated 4 Å molecular sieves. Anhydrous acetonitrile was dried and deoxygenated on a Glass Contour System (Pure Process Technology, LLC) and stored over activated 4 Å molecular sieves. $[^nBu_4N][BH_4]$ and V_2O_5 were purchased from Sigma-Aldrich and used as received. The supporting electrolyte $[^nBu_4N][PF_6]$ was purchased from Sigma-Aldrich, recrystallized three times using hot methanol, and stored under dynamic vacuum for a minimum of two days prior to use. $VO(O^tBu)_3$ and $VO(OCH_3)_3$ were synthesized according to the literature.[1]

Mass spectrometry analyses were performed on an Advion expression^L Compact Mass Spectrometer equipped with an electrospray probe and an ion-trap mass analyzer. Direct injection analysis was employed in all cases with a sample solution in acetonitrile. ^{1}H NMR spectra were recorded at 500 on Bruker DPX-500 spectrometer locked on the signal of deuterated solvents. All chemical shifts were reported relative to the peak of residual ^{1}H signal in deuterated solvents. CD_3CN was purchased from Cambridge Isotope Laboratories, degassed by three freeze−pump−thaw cycles, and stored over activated 4 Å molecular sieves. Infrared (FT-IR, ATR) spectra of complexes were recorded on a Shimadzu IRAffinity-1 Fourier Transform Infrared Spectrophotometer and are reported in wavenumbers (cm^{-1}). Electronic absorption measurements were recorded at room temperature in anhydrous acetonitrile in a sealed 1 cm quartz cuvette with an Agilent Cary 60 UV-Vis spectrophotometer. Single crystals were mounted on the tip of a thin glass optical fiber (goniometer head) and mounted on a Bruker SMART APEX II CCD platform diffractometer for a data collection at 100.0(5) K. The structures were solved using SHELXT-2014/5[2] and refined using SHELXL-2014/7.[3]

Cyclic Voltammetry. Concentrations of active species (vanadium cluster) and $[^nBu_4N][PF_6]$ used were 1 mM and 100 mM, respectively. CV measurements were carried out using a Bio-Logic VMP3 potentiostat/galvanostat and the EC-Lab software suite. Glassy carbon discs (3 mm, CH Instruments, USA) were used as working electrodes. Working electrodes were polished using a micro cloth pad and 0.05 μM alumina powder. Potentials recorded during CV were measured relative to a nonaqueous Ag/Ag^+ reference electrode with 10 mM $AgNO_3$ and 100 mM $[^nBu_4N][PF_6]$ in acetonitrile (Bio-Logic). A platinum wire served as the counter electrode. All experiments were carried out at room temperature inside a nitrogen-filled glove box (MBraun, USA). All CV measurements were iR compensated at 85% with impedance taken at 100kHz using the ZIR tool included with the EC-Lab software.

Determining D_0 and k_0. Concentrations of active species (vanadium cluster) used were 1 mM with 0.1 M $[^nBu_4N][PF_6]$ supporting electrolyte. CV measurements were carried out inside a nitrogen filled glove box (MBraun, USA) using a Bio-Logic VMP3 potentiostat/galvanostat and the EC-Lab software suite. Cyclic voltammograms were recorded using a 3 mm diameter glassy carbon working electrode (CH Instruments, USA), a Pt wire auxiliary electrode (CH Instruments, USA), and a Ag/Ag^+ non-aqueous reference electrode with 0.01 M $AgNO_3$ in 0.1 M $[^nBu_4N][PF_6]$ in CH_3CN (Bio-Logic). Cyclic voltammograms were *iR* compensated at 85% with impedance taken at 100 kHz using the ZIR tool included in the EC-Lab software.

The diffusion coefficient associated with each neutral cluster was determined by using the slope of the peak current (i_p) of the oxidative wave (cathodic sweep) versus the square root of scan rate $\nu^{1/2}$. The Randles-Sevcik equation was used to estimate the diffusion coefficients from CV data. For a reversible redox couple, the peak current is given by the eq. S1;

$$i_p = 2.69 \times 10^5 n^{3/2} A\, c\, D_0^{1/2} \nu^{1/2} \quad \text{Eq. S1}$$

In eq. S1, n is the number of electrons transferred; A is the electrode area (0.0707 cm^2 for the glassy carbon working electrode); c is the bulk concentration of the active species; D_0 is the diffusion coefficient of the active species; ν is the scan rate. For an irreversible redox couple, the peak current, is given by the eq. S2:

$$i_p = 2.99 \times 10^5 n^{3/2} \alpha^{1/2} A\, c\, D_0^{1/2} \nu^{1/2} \quad \text{Eq. S2}$$

where α is the charge transfer coefficient (α ~ 0.5).

For the redox couples that show quasi-reversible kinetics, relationships for both reversible and irreversible redox reaction are usually employed to determine the diffusion coefficients of such redox processes. Therefore, an average value of diffusion coefficient was approximated for a quasi-reversible redox couple using both equations S1 and S2.[4-6]

The Heterogeneous Electron-Transfer Rate Constants were calculated using the Nicholson method.[7] The potential difference (ΔEp) of oxidation and reduction peaks were obtained at different scan rates. The transfer parameter, ψ, was extracted from the working curve constructed by Nicholson using ΔEp values. The standard heterogeneous charge-transfer rate constant, k_0, for a given electron transfer process was determined using the following equation:

$$\psi = \frac{k_0}{(\frac{\pi n F D \nu}{RT})^{1/2}} \quad \text{Eq. 3}$$

where n is the number of electrons transferred, F is the Faraday constant, D is the diffusion coefficient, v is the scan rate, R is the ideal gas constant and T is the temperature.[7, 8]

Parameters for chronoamperometry/bulk electrolysis experiments. Bulk electrolysis experiments were performed in a H-cell with a glass frit separator (Porosity =10-16 µm, Pine Research, USA) using a Bio-Logic VMP3 potentiostat/galvanostat. An active species concentration of 1 mM was used. Working electrode compartment contained 15 mL of the active species with 100 mM [^{n}Bu$_4$N][PF_6] in CH_3CN and counter electrode compartment had 15 mL of 100 mM [^{n}Bu$_4$N][PF_6] in CH_3CN. A Pt mesh working electrode and a Pt wire counter electrode were used. Bulk electrolysis experiments were carried out using the chronoamperometry techniques available in EC lab software suite at constant potentials, selected from CV.

Parameters for static H-cell charge discharge experiments. Charge-discharge testing was carried out inside a nitrogen filled glove box (MBraun, USA) using a glass H-cell separated by a microporous glass frit (P5, 1.6 µm, Adams and Chittenden, USA). Each compartment contained stirring solutions (5 mL), with 1 mM active species and 100 mM [^{n}Bu$_4$N][PF_6] in acetonitrile. Two graphite felt electrodes (1 × 1 × 0.5 cm, Fuel Cell Store, USA) were attached to Pt wire current collectors and submerged in the posolyte and negolyte chambers (~0.5 cm), where they were allowed to soak for 1 hour prior to the start of the experiment. Experiments were conducted using a Bio-Logic VMP3 potentiostat/galvanostat with galvanostatic charging and discharging conditions at 0.1 mA. Voltage limits of 2.5 V and 0.1 V were applied for cycling.

Parameters for flow cell experiments. Laboratory-scale RFBs (Fuel Cell Technologies, Albuquerque, NM, USA) were assembled using 5 mL 20 mM 2-EE catholyte and anolyte, supported in 0.1 M [^{n}Bu$_4$N][PF$_6$] in acetonitrile in a glovebox under UHP argon. The RFB was run at 25 °C, and two peristaltic pumps (Masterflex L/S) passed electrolyte at 2.5 mL min^{-1} from polypropylene reservoirs through norprene tubing into a serpentine flow field past a 5 cm^2 active membrane area. A Solartron 1287 potentiostat/galvanostat applied a 10 mA charge/discharge current across two carbon felt electrodes (SGL carbon, GFD grade, 2.5 mm nominal thickness, 5 cm^2 active area) compressed to 80% of their original thickness situated on opposing sides of 20 sheets of Tonen E20MMS separator. Voltage limits of 2.5 and 0.05 V were applied for the experiment.

Cell performance can also be characterized with the "electrochemical yield," which is defined here as the observed capacity during charge or discharge divided by the theoretical capacity. Theoretical capacity is calculated using the solution concentration, solution volume, and the number of electrons transferred per molecule of active material. Coulombic efficiency is calculated by dividing discharge capacity by charge capacity.

Synthesis of $[V_6O_7(OC_2H_4OCH_3)_{12}]$ (1) and Synthesis of $[V_6O_7(OC_2H_4OC_2H_5)_{12}]$ (2).
In the glovebox, $VO(O^tBu)_3$ (0.250 g, 0.9 mmol), $[^nBu_4N][BH_4]$ (0.075 g, 0.3 mmol), and the respective alcohol R-OH (8 mL, R = $C_2H_4OCH_3$ or $C_2H_4OC_2H_5$) were charge in a 25 mL Teflon-lined autoclave (PARR). The steel reaction vessel was sealed, and the mixture heated to 125 °C for 24 h. After the allotted time period, the autoclave was cooled to room temperature, and the subsequent workup completed in ambient atmosphere. The resulting green solution was dried under reduced pressure to obtain a dark green oil, identified as the respective anionic clusters $[^nBu_4N][V_6O_7(OR)_{12}]$. Oxidation to form the neutral cluster was accomplished by adding a solution of I_2 (0.050 g, 0.197 mmol) in acetonitrile (20 mL) to the crude solid with stirring overnight. The acetonitrile was removed under reduced pressure and the products $[V_6O_7(OC_2H_4OCH_3)_{12}]$ (**1**) or $[V_6O_7(OC_2H_4OC_2H_5)_{12}]$ (**2**) extracted with hexanes for use.

$[V_6O_7(OC_2H_4OCH_3)_{12}]$ (7). Appearance: dark green oil at room temperature. Yield: 0.092 g, 0.07 mmol, 48 %. UV−Vis (CH_3CN) [ε (M^{-1} cm^{-1})]: 396 nm (6.32 x 10^3), 1000 nm (1.21 x 10^3). ESI-MS (+): *m/z* 1318. X-ray quality crystals were generated *via* reduction of the crude, anionic complex $[V_6O_7(OC_2H_4OCH_3)_{12}]^-$ with tetrabutylammonium hydroxide in acetonitrile. Following gentle heating of the reaction mixture (40 °C) for two hours, the solution turned from green to blue-green, indicating reduction to the di-anionic charge state, $[V_6O_7(OC_2H_4OCH_3)_{12}]^{2-}$. This solution was condensed to one-third its original volume, and cooled to −35 °C. After approximately eight weeks, blue-green crystals of $[V_6O_7(OC_2H_4OCH_3)_{12}]^{2-}$ were isolated. Refinement of the data revealed the expected Lindqvist structure with six vanadyl moieties and twelve bridging $-OC_2H_4OCH_3$ groups (Figure S4, Table S1).

$[V_6O_7(OC_2H_4OC_2H_5)_{12}]$ (8). Appearance: dark green oil at room temperature. Yield: 0.123 g, 0.08 mmol, 57 %. UV−Vis (CH_3CN) [ε (M^{-1} cm^{-1})]: 396 nm (4.88 x 10^3), 1000 nm (9.97 x 10^2). ESI-MS (+): *m/z* 1487.

Synthesis of heteroleptic "mixed" POV-alkoxides, $V_6O_7(OR)_{12-x}(OCH_3)_x$
R = $C_2H_4OCH_3$ (1-Mixed), $C_2H_4OC_2H_5$ (2-Mixed).
In the glovebox, $VO(OCH_3)_3$ (0.300 g, 1.9 mmol), $[^nBu_4N][BH_4]$ (0.080 g, 0.3 mmol), and the respective alcohol R-OH (8 mL, R = $C_2H_4OCH_3$, $C_2H_4OC_2H_5$) were charge in a 25 mL Teflon-lined autoclave (PARR). The reaction vessel was sealed, and the mixture heated to 125 °C for 24 h. After the allotted time period, the autoclave was cooled to room temperature, and the subsequent workup completed in ambient atmosphere. The resulting green solution was dried under reduced pressure to obtain the crude products, identified as the respective anionic clusters $[^nBu_4N][V_6O_7(OR)_{12-x}(OCH_3)_x]$. Oxidation to form the neutral cluster was accomplished by adding a solution of I_2 (0.050 g, 0.197 mmol) in acetonitrile (20 mL) to the crude solid with stirring overnight. The acetonitrile was removed under reduced pressure and the products extracted with hexanes for use. Yields for mixtures calculated using average product mass from ESI-MS data.

$[V_6O_7(OC_2H_4OCH_3)_{12-x}(OCH_3)_x]$ (1-Mixed). Appearance: Dark green oil at room temperature. Yield: 0.315 g, 0.27 mmol, 85 %. UV−Vis (CH_3CN) [ε (M^{-1} cm^{-1})]: 392 nm (6.48 x 10^3), 1000 nm (7.65 x 10^2). ESI-MS (+*ve*): *m/z* = 1318 $[V_6O_7(OC_2H_4OCH_3)_{12}]$, *m/z* = 1274 $[V_6O_7(OC_2H_4OCH_3)_{11}(OCH_3)_1]$, *m/z* = 1231 $[V_6O_7(OC_2H_4OCH_3)_{10}(OCH_3)_2]$, *m/z* = 1187 $[V_6O_7(OC_2H_4OCH_3)_9(OCH_3)_3]$, *m/z* = 1142 $[V_6O_7(OC_2H_4OCH_3)_8(OCH_3)_4]$.

$[V_6O_7(OC_2H_4OC_2H_5)_{12-x}(OCH_3)_x]$ (2-Mixed). Appearance: Dark green oil at room temperature. Yield: 0.341 g, 0.27 mmol, 87 %. UV−Vis (CH_3CN) [ε (M^{-1} cm^{-1})]: 392 nm (6.03 x 10^3), 1000 nm (6.30 x 10^2). ESI-MS (+*ve*): *m/z* = 1487 $[V_6O_7(OC_2H_4OC_2H_5)_{12}]$, *m/z* = 1429 $[V_6O_7(OC_2H_4OC_2H_5)_{11}(OCH_3)_1]$, *m/z* = 1371 $[V_6O_7(OC_2H_4OC_2H_5)_{10}(OCH_3)_2]$, *m/z* = 1313 $[V_6O_7(OC_2H_4OC_2H_5)_9(OCH_3)_3]$, *m/z* = 1255 $[V_6O_7(OC_2H_4OC_2H_5)_8(OCH_3)_4]$, *m/z* = 1197 $[V_6O_7(OC_2H_4OC_2H_5)_7(OCH_3)_5]$, *m/z* = 1138 $[V_6O_7(OC_2H_4OC_2H_5)_6(OCH_3)_6]$.

Figure S1. ESI-MS (+*ve*) of (a) **1** and (b) **2**

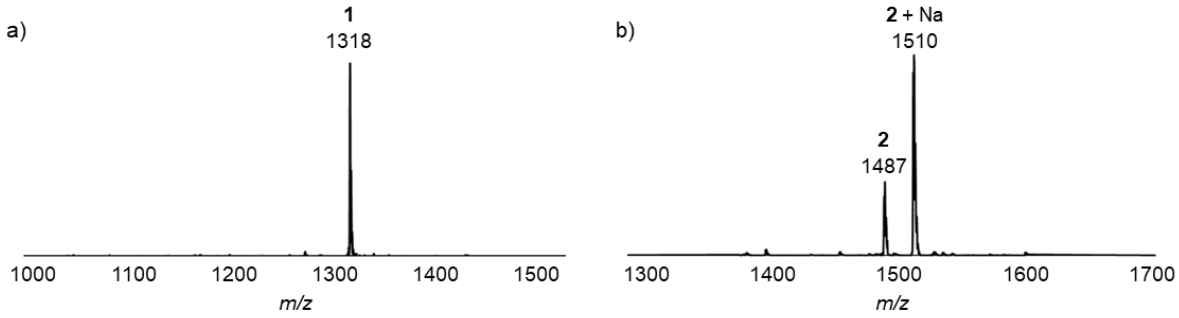

Figure S2. ^{1}H NMR of **1** and **2** in CD_3CN

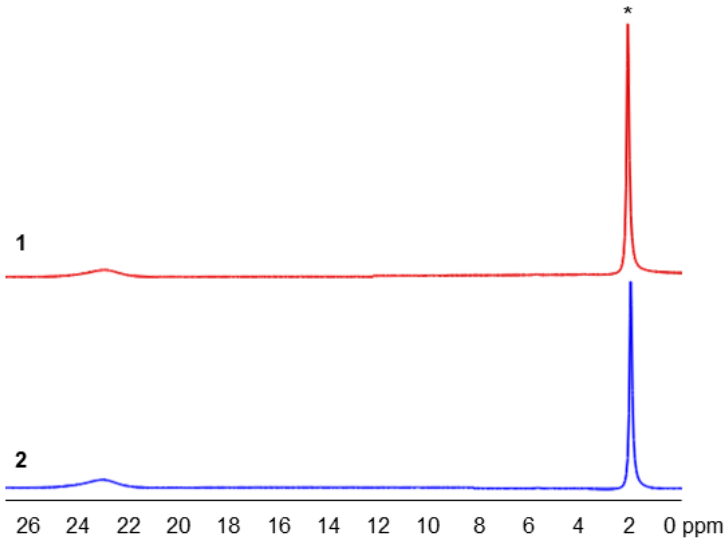

Figure S3. Electronic absorption spectra of **1**, **2**, **1-Mixed**, and **2-Mixed** recorded in acetonitrile. Inset shows low energy region.

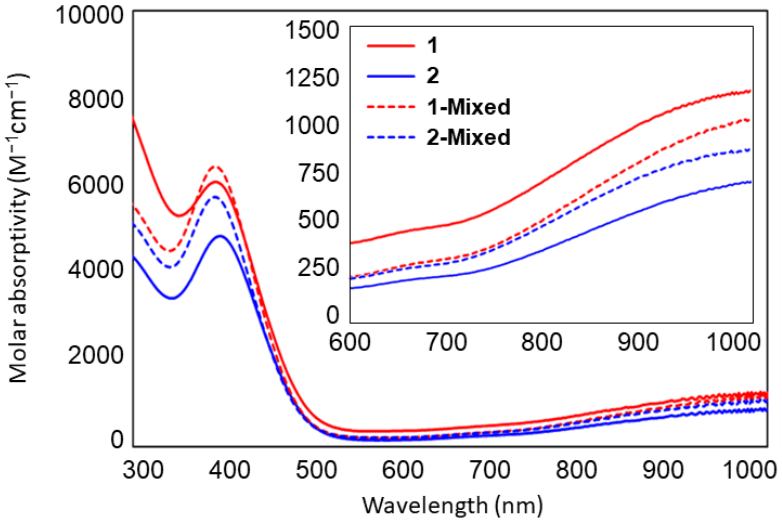

Table S1. Crystallographic parameters for molecular structure of $[V_6O_7(OC_2H_4OCH_3)_{12}]^{2-}$

Compound	$[V_6O_7(OC_2H_4OCH_3)_{12}]^{2-}$ **CCDC** 1907800
Empirical formula	$C_{68}H_{156}N_2O_{31}V_6$
Formula weight	1803.58
Temperature / K	222.99(10)
Wavelength / Å	1.54184
Crystal system	monoclinic
Space group	$P2_1/n$
Unit cell dimensions	a = 15.12380(10) Å b = 17.5194(2) Å c = 17.40260(10Å α = 90° β = 97.4030(10)° γ = 90°
Volume / Å^3	4572.56(7) Å^3
Z	2
Reflections collected	45341
Independent reflections	9586
Completeness (theta)	99.7% (74.504°)
Goodness-of-fit on F^2	1.070
Final R indices [I>2sigma(I)]	$R1$ = 0.0385
Largest diff. peak and hole	0.469 and -0.403 e.Å^{-3}

Figure S4. Molecular structure of $[V_6O_7(OC_2H_4OCH_3)_{12}]^{2-}$ shown with 50 % probability ellipsoids. Hydrogen atoms and counter ions [^{n}Bu$_4$N] eliminated for clarity.

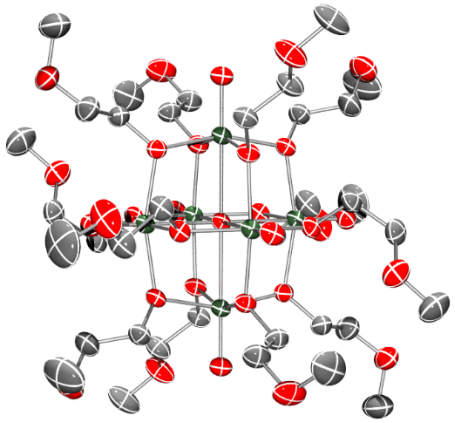

Figure S5. Beer's Law plots and solubility calculations for complex **1** in MeCN with 0.1 M [^{n}Bu$_4$N][PF$_6$]. Absorption spectra blanked with 0.1 M [^{n}Bu$_4$N][PF$_6$].

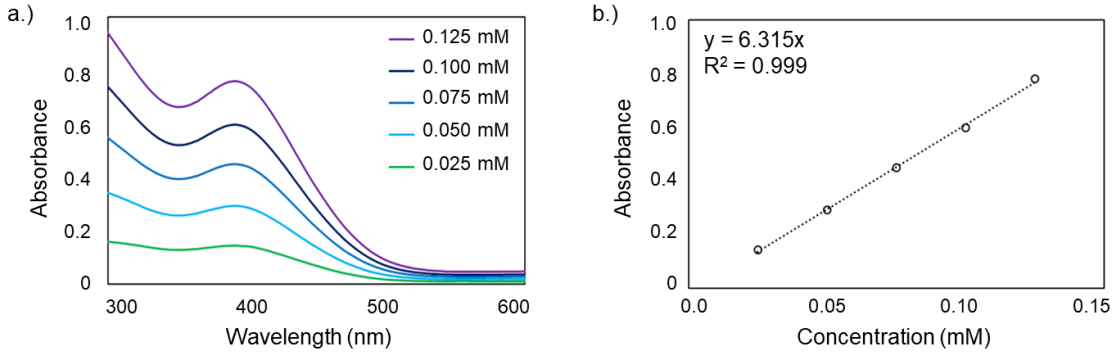

Trial	Absorbance (396 nm)	Dilute Conc. (mM)	Dilution	Saturated Concentration (M)
1	0.8753	0.1386	15 µL to 100 mL	0.924
2	0.8819	0.1397	15 µL to 100 mL	0.931
3	0.8961	0.1419	15 µL to 100 mL	0.946

Average Concentration of 1 = 0.934 ± 0.011 M

Figure S6. Beer's Law plots and solubility calculations for complex **2** in MeCN with 0.1 M [^{n}Bu$_4$N][PF$_6$]. Absorption spectra blanked with 0.1 M [^{n}Bu$_4$N][PF$_6$].

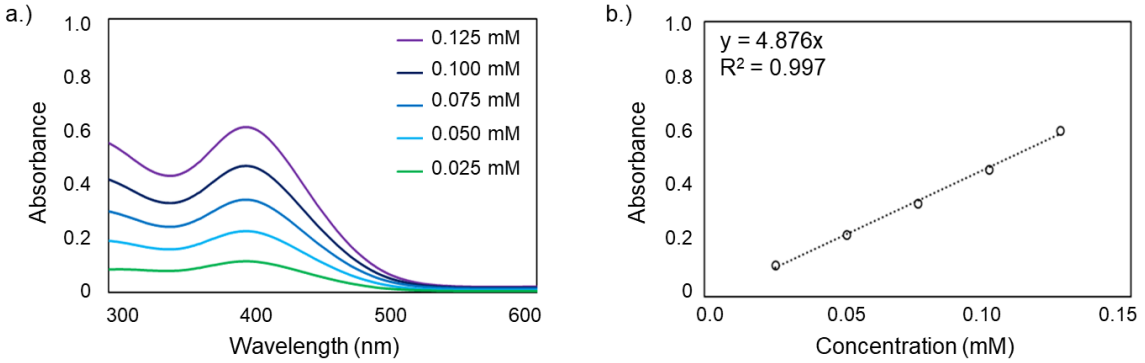

Trial	Absorbance (396 nm)	Dilute Conc. (mM)	Dilution	Saturated Concentration (M)
1	0.6744	0.1383	15 µL to 100 mL	0.922
2	0.6875	0.1410	15 µL to 100 mL	0.940
3	0.6641	0.1362	15 µL to 100 mL	0.908

Average Concentration of 2 = 0.923 ± 0.016 M

Figure S7. CVs **1**, **2**, **1-Mixed**, and **2-Mixed** in MeCN with 0.1 M [^{n}Bu$_4$N][PF$_6$]. Recorded at 100 mV/s

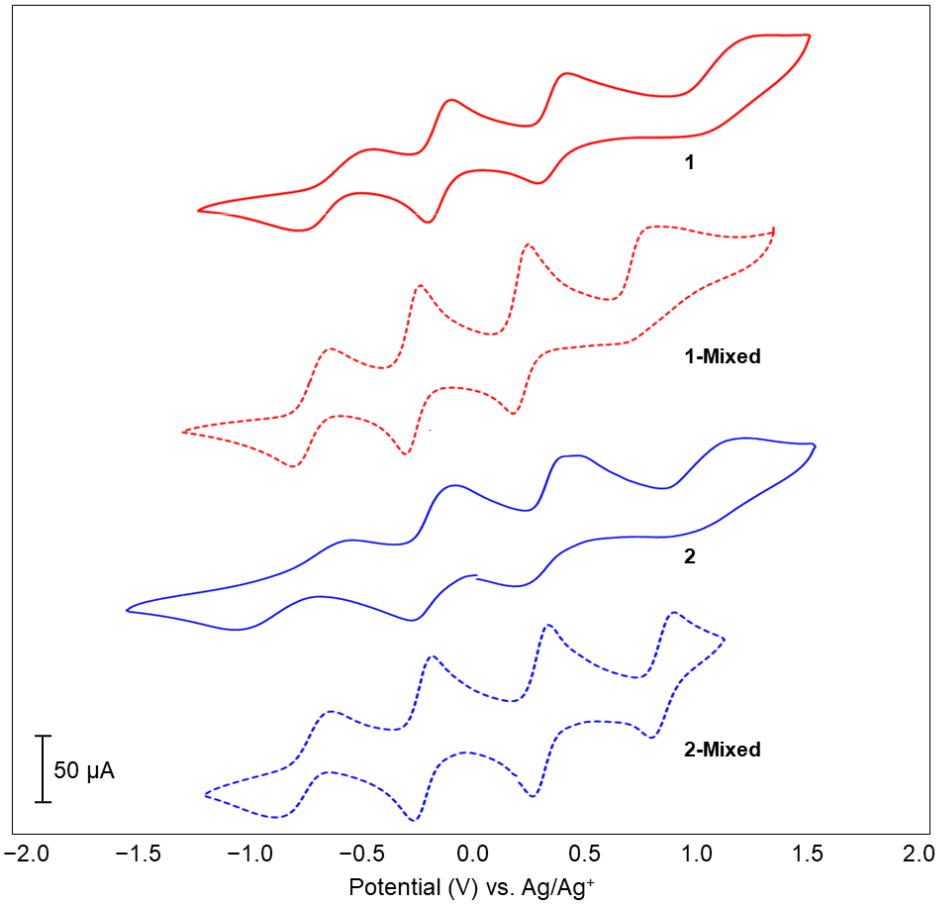

Figure S8. CVs of solutions of (a) **1** and (b) **2** before and after bulk reduction and oxidation.

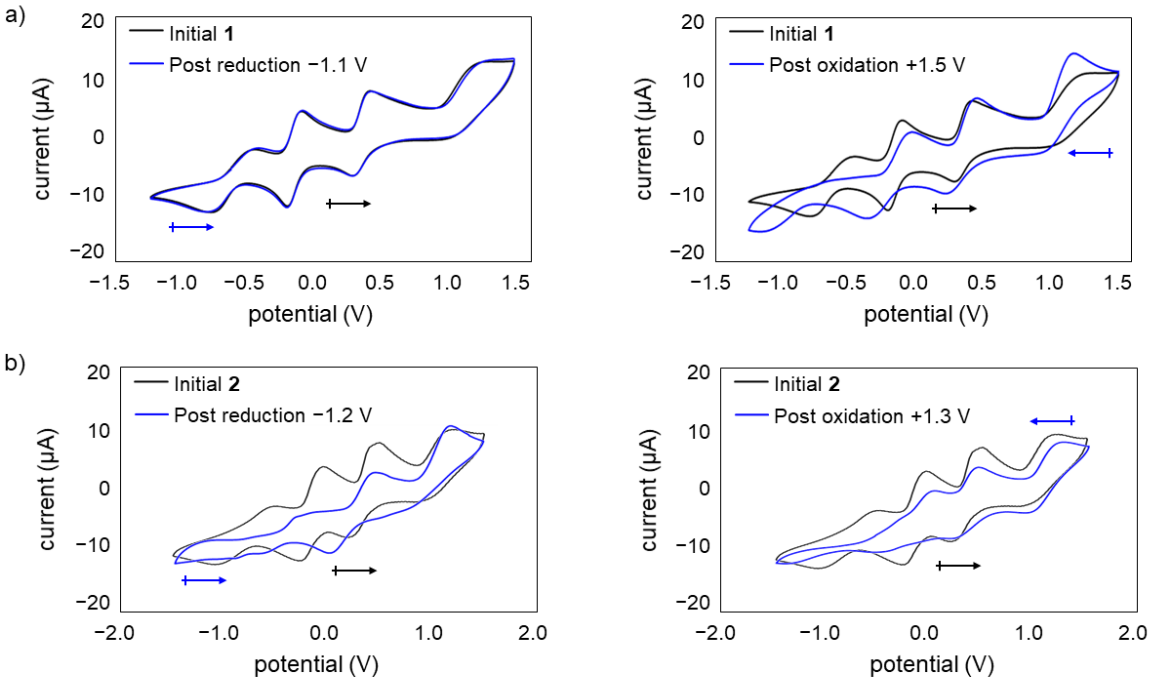

Figure S9. ESI-MS (+*ve*) of (a) **1-Mixed** and (b) **2-Mixed**

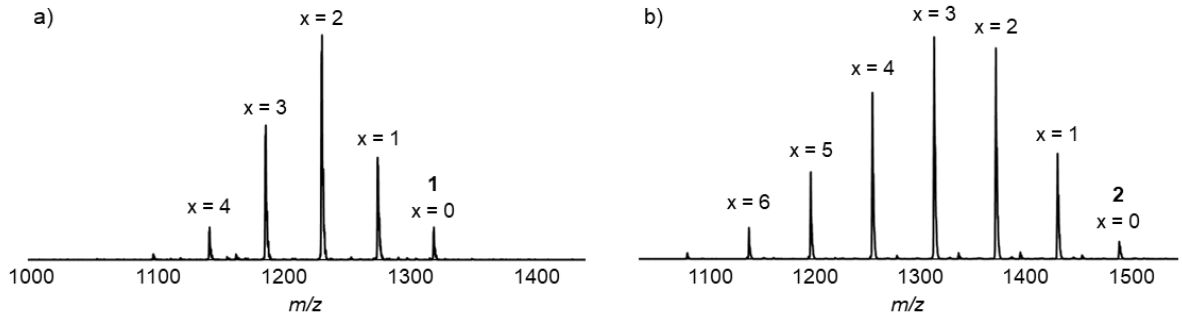

Figure S10. ^{1}H NMR of **1-Mixed** and **2-Mixed** in CD_3CN

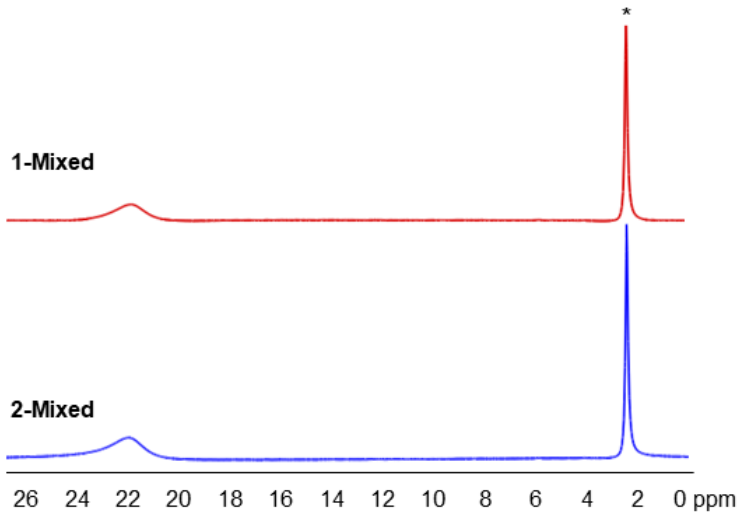

Figure S11. Beer's Law plots and solubility calculations for **1-Mixed** in MeCN with 0.1 M [^{n}Bu$_4$N][PF$_6$]. Absorption spectra blanked with 0.1 M [^{n}Bu$_4$N][PF$_6$].

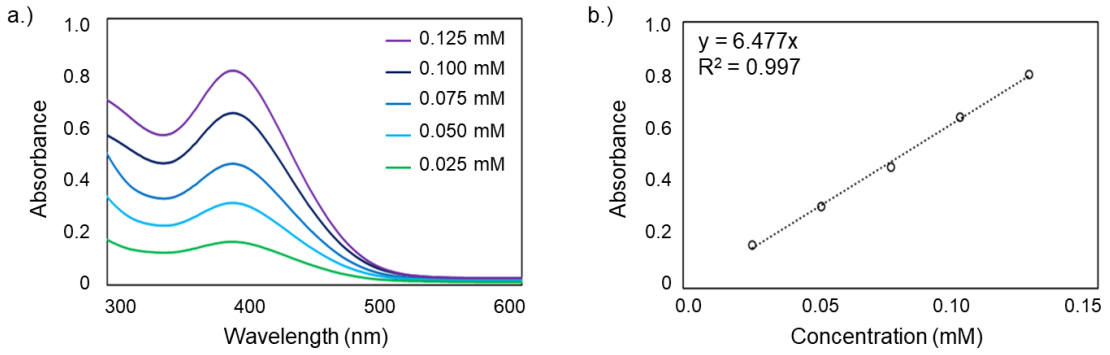

Trial	Absorbance (392 nm)	Dilute Conc. (mM)	Dilution	Saturated Concentration (M)
1	0.7377	0.1139	5 µL to 10 mL, 1 mL to 5 mL	1.139
2	0.7672	0.1185	5 µL to 10 mL, 1 mL to 5 mL	1.185
3	0.7768	0.1200	5 µL to 10 mL, 1 mL to 5 mL	1.199

Average Concentration of 1-Mixed = 1.174 ± 0.031 M

Figure S12. Beer's Law plots and solubility calculations for **2-Mixed** in MeCN with 0.1 M [^{n}Bu$_4$N][PF$_6$]. Absorption spectra blanked with 0.1 M [^{n}Bu$_4$N][PF$_6$].

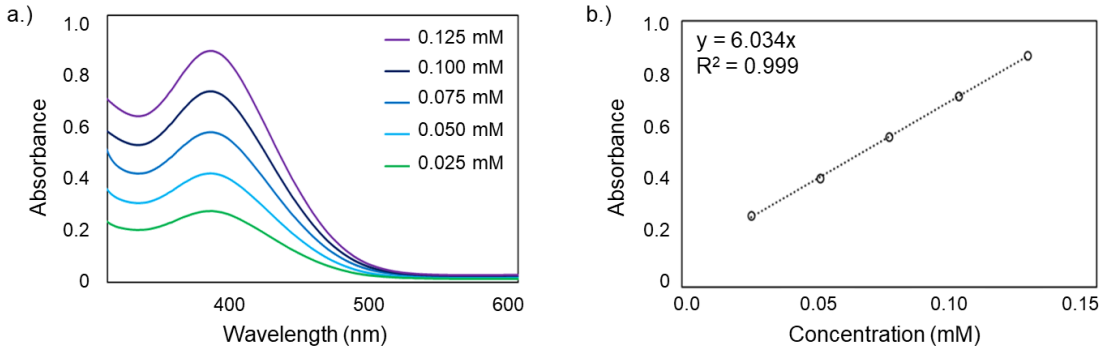

Trial	Absorbance (392 nm)	Dilute Conc. (mM)	Dilution	Saturated Concentration (M)
1	0.5742	0.0952	5 µL to 10 mL, 1 mL to 5 mL	0.952
2	0.5822	0.0965	5 µL to 10 mL, 1 mL to 5 mL	0.965
3	0.5742	0.0952	5 µL to 10 mL, 1 mL to 5 mL	0.952

Average Concentration of 2-Mixed = 0.956 ± 0.008 M

Figure S13. Plots of i_p vs. $\sqrt{v}$ and ΔE vs. v for (a) **1**, (b) **1-Mixed**, and (c) **2-Mixed**

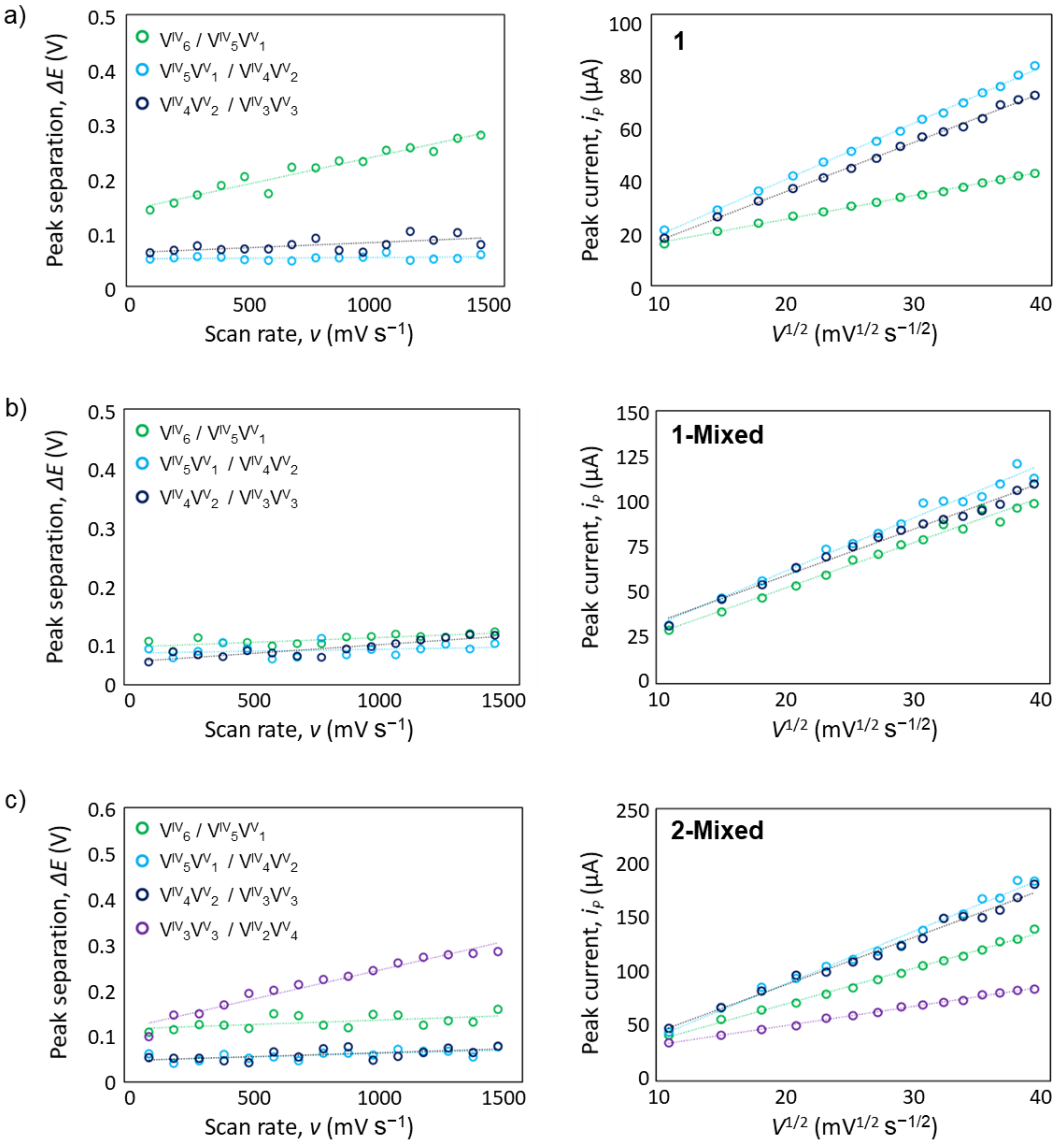

Table S2. Diffusion coefficients (D_0) and heterogeneous electron transfer rate constants (k_0) for each redox event of **1**, **2**, **1-Mixed**, and **2-Mixed**

		$V^{IV}_6/V^{IV}_5V^{V}_1$ couple	$V^{IV}_5V^{V}_1/V^{IV}_4V^{V}_2$ couple	$V^{IV}_4V^{V}_2/V^{I}_3V^{V}_3$ couple	$V^{IV}_3V^{V}_3/V^{IV}_4V^{V}_2$ couple
Complex	D_0 ($cm^2\ s^{-1}$)	k_0 ($cm\ s^{-1}$)	k_0 ($cm\ s^{-1}$)	k_0 ($cm\ s^{-1}$)	k_0 ($cm\ s^{-1}$)
1	3.10×10^{-6}	3.62×10^{-3}	2.88×10^{-2}	9.40×10^{-2}	*b*
2	*a*	*a*	*a*	*a*	*a*
1-Mixed	2.69×10^{-5}	6.20×10^{-2}	4.33×10^{-1}	3.62×10^{-1}	*a*
2-Mixed	7.63×10^{-5}	1.68×10^{-2}	9.85×10^{-1}	7.65×10^{-1}	5.11×10^{-3}

[a]For complex **2**, redox processes become poorly defined at scan rates exceeding 300 mV/s, making it impossible to calculate either k_0 or D_0 using these methods.

[b]For both **1** and **1-Mixed**, k_0 values could not be determined for the most oxidizing event, $V^{IV}_3V^{V}_3/V^{IV}_4V^{V}_2$, as the peak became irreversible at potentials >300 mV/s, making determining ΔE impossible.

Figure S14. CVs of solutions of **1-Mixed** and (b) **2-Mixed** before and after bulk reduction and oxidation.

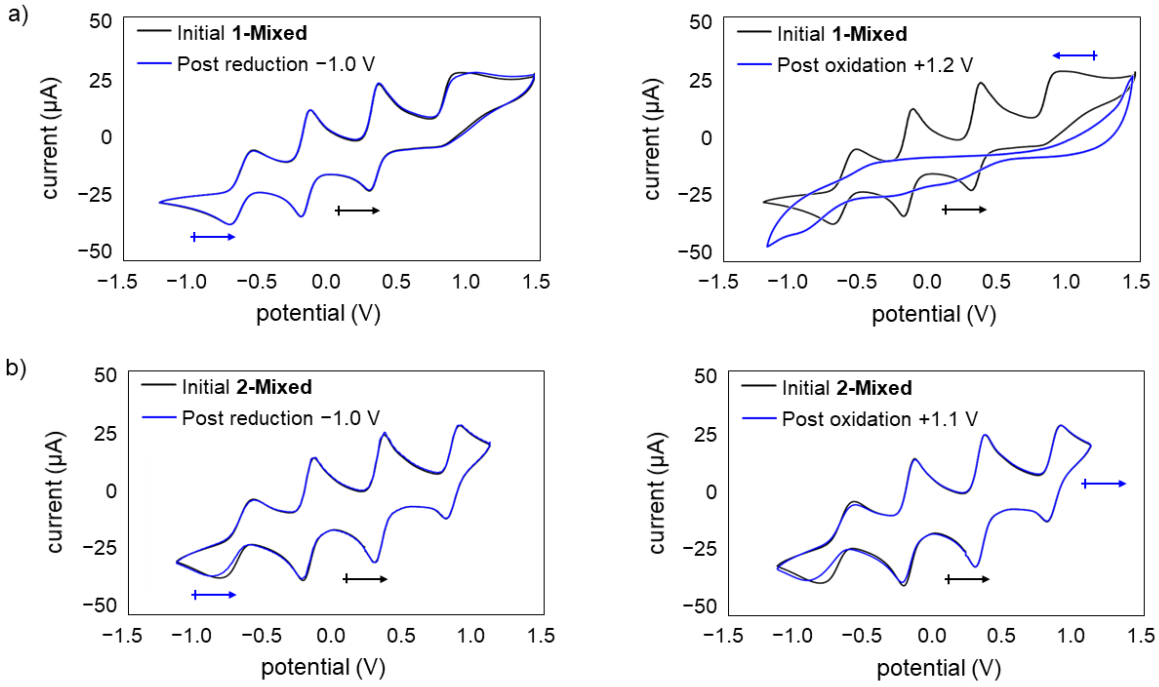

Figure S15. (top) Potential versus time of static H-cell charge-discharge with **2-Mixed**. (bottom left) Potential versus capacity and (bottom right) coulombic efficiency for all 30 cycles.

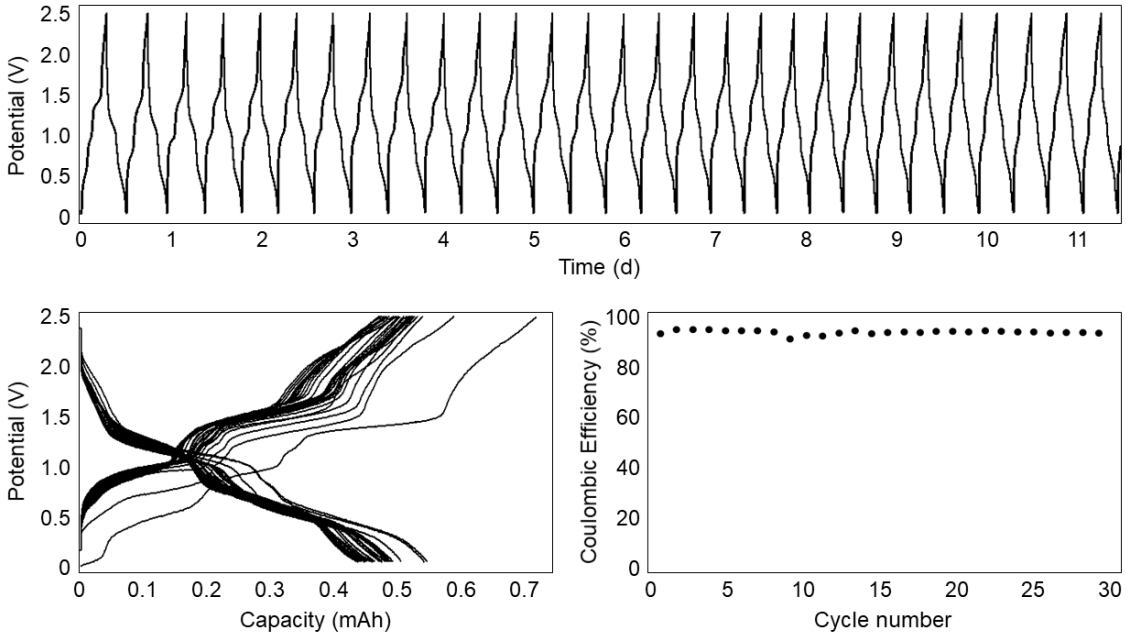

Figure S16. CVs of solutions of **2-Mixed** before and after static H-cell charge discharge.

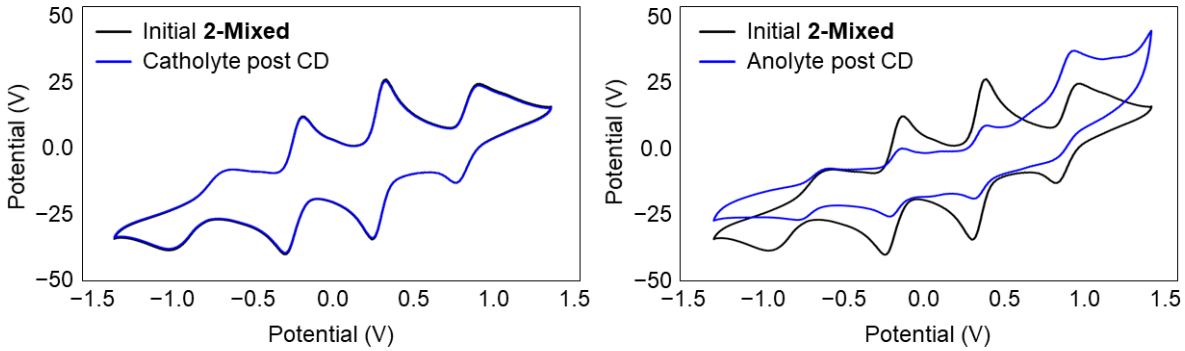

Figure S17. Potential versus time for 20 flow cycles of **2-Mixed**

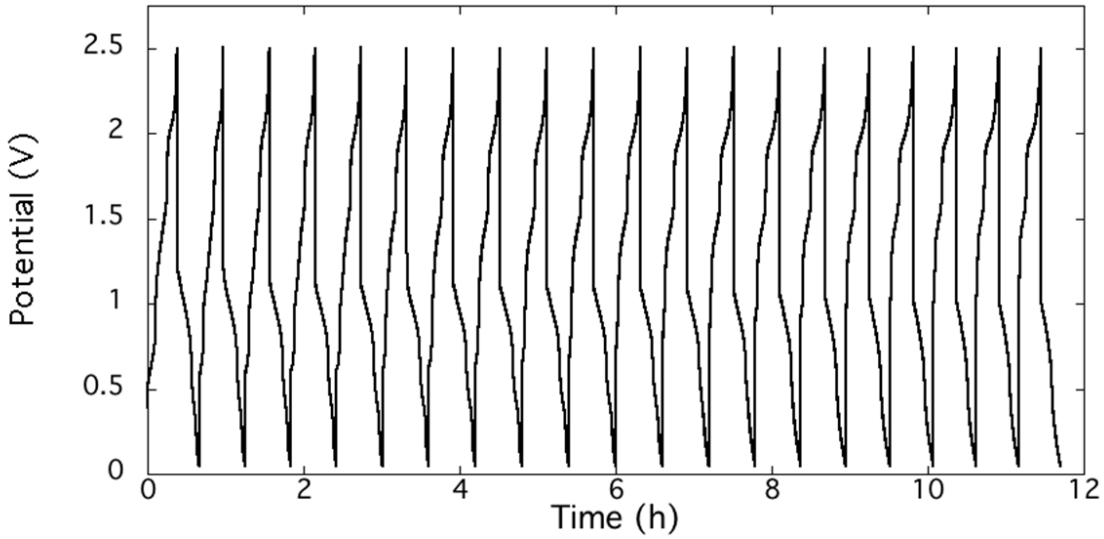

Figure S18. Potential versus capacity for 20 flow cycles of **2-Mixed**

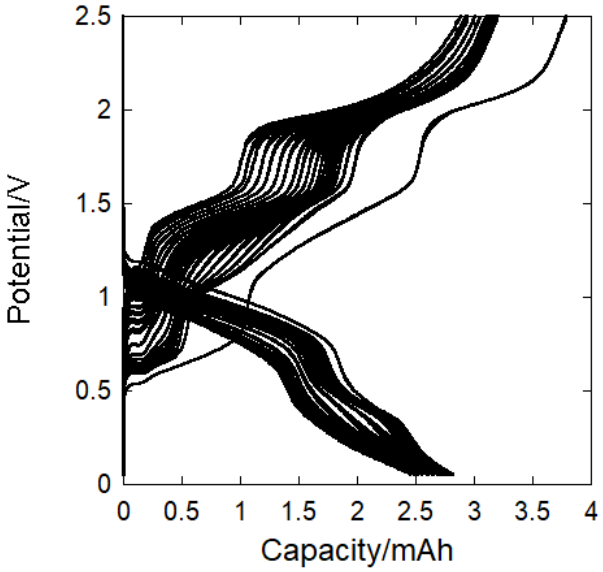

Figure S19. Coulombic efficiency (left) and electrochemical yield (right) for 20 flow cycles of **2-Mixed**

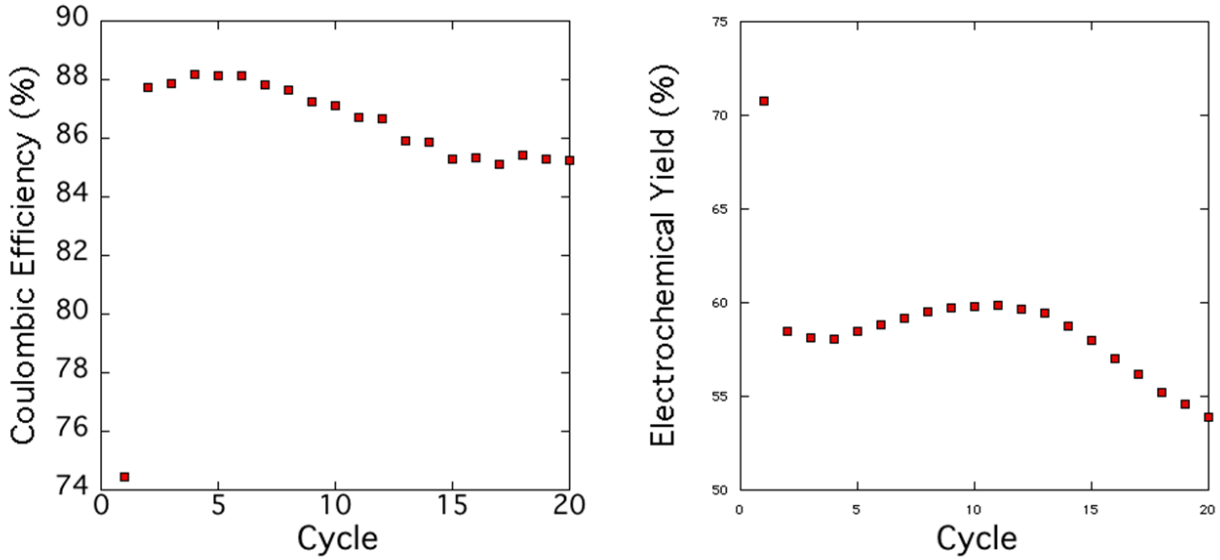

Figure S20. CV of anolyte and catholyte solutions following 20 charge-discharge flow cycles of **2-Mixed**

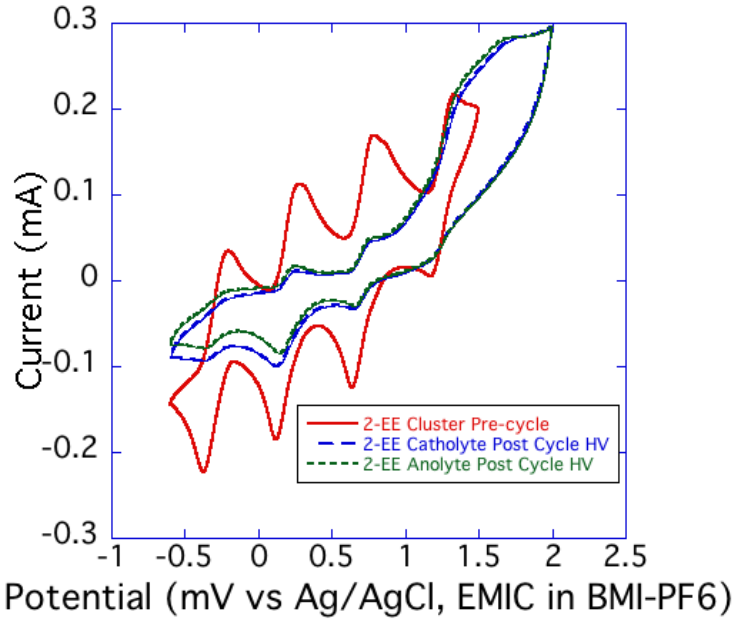

References.

1. C. Daniel and H. Hartl, *Journal of the American Chemical Society*, 2009, **131**, 5101-5114.
2. G. M. Sheldrick, *SHELXT-2014/5*.
3. G. M. Sheldrick, *Acta Crystallographica Section C*, **71**, 3-8.
4. Q. Liu, A. E. S. Sleightholme, A. A. Shinkle, Y. Li and L. T. Thompson, *Electrochemistry Communications*, 2009, **11**, 2312-2315.
5. A. E. S. Sleightholme, A. A. Shinkle, Q. Liu, Y. Li, C. W. Monroe and L. T. Thompson, *Journal of Power Sources*, 2011, **196**, 5742-5745.
6. A. M. Kosswattaarachchi, A. E. Friedman and T. R. Cook, *ChemSusChem*, 2016, **9**, 3317-3323.
7. R. S. Nicholson and I. Shain, *Analytical Chemistry*, 1964, **36**, 706-723.
8. H. Muhammad, I. A. Tahiri, M. Muhammad, Z. Masood, M. A. Versiani, O. Khaliq, M. Latif and M. Hanif, *Journal of Electroanalytical Chemistry*, 2016, **775**, 157-162.